Restor Dent Endod. 2024 Nov;49(4):e37
https://doi.org/10.5395/rde.2024.49.e37
eISSN 2234-7666

Restorative Dentistry & Endodontics RDE

Research Article

Check for updates

Physical-mechanical, chemical and biological properties of graphene-reinforced glass ionomer cements

Tatiane Ramos dos Santos Jordão,[1] **Laura Soares Viana Fernandes**,[1] **Karla Lorene de França Leite**,[2] **Adílis Alexandria**,[1] **Emmanuel João Nogueira Leal Silva**,[3] **Lucianne Cople Maia**,[2] **Tatiana Kelly da Silva Fidalgo**[1*]

[1]Department of Preventive and Community Dentistry, Dental School, Universidade do Estado do Rio de Janeiro, Rio de Janeiro, Brazil
[2]Department of Pediatric Dentistry and Orthodontics, Dental School, Universidade Federal do Rio de Janeiro, Rio de Janeiro, Brazil
[3]Department of Clinics, Dental School, Universidade do Estado do Rio de Janeiro, Rio de Janeiro, Brazil

OPEN ACCESS

Received: Apr 22, 2024
Revised: Aug 7, 2024
Accepted: Aug 7, 2024
Published online: Oct 10, 2024

Citation
Jordão TRS, Fernandes LSV, Leite KLF, Alexandria A, Silva EJN, Maia LC, *et al*. Physical-mechanical, chemical and biological properties of graphene-reinforced glass ionomer cements. Restor Dent Endod 2024;49(4):e37.

***Correspondence to**
Tatiana Kelly da Silva Fidalgo, PhD
Department of Preventive and Community Dentistry, Dental School, Universidade do Estado do Rio de Janeiro, Av. 28 de Setembro, 157 – Vila Isabel, Rio de Janeiro 20551-030, Brazil.
Email: tatianaksfidalgo@gmail.com

Funding
The authors acknowledge the Fundação de Amparo à Pesquisa do Estado do Rio de Janeiro (FAPERJ) (241735/2018) for the

ABSTRACT

Objectives: This study aimed to evaluate the physical-mechanical, chemical, and biological properties of graphene-reinforced glass ionomer cements (GICs).
Materials and Methods: Different proportions of graphene powder were incorporated into 2 high-viscosity self-curing GIC, Ketac Molar (G_{Ketac}) and Fuji IX (G_{Fuji}), in 4 different concentrations: 0.5%, 1%, 2%, and 5%. The control groups included the GICs without graphene. Experiments were performed to analyze linear (Ra) and volumetric roughness (Sa), antimicrobial activity, radiopacity, fluoride release, microhardness, solubility, and water sorption. Data were analyzed using Kruskal-Wallis, Mann-Whitney, Wilcoxon, analysis of variance, and Tukey's test ($p \leq 0.05$).
Results: The G_{Ketac} 0% and G_{Fuji}0% groups presented higher Ra (4.05 and 2.72) and Sa (4.76 and 5.16), respectively. No inhibition zone was observed, and the incorporation of graphene reduced radiopacity. Moreover, there was no influence on the solubility and water sorption after 21 days. A greater fluoride release was observed in the period of 7 days for most of the groups. After 21 days, G_{Ketac} 5%, 2%, and 1% presented higher releasing than 0% and 0.5% ($p \leq 0.05$).
Conclusions: The graphene incorporation improved the microhardness of GICs in lower concentrations. Graphene incorporation to GICs modified some physical-mechanical, and chemical, but not affected biological properties.

Keywords: Dental materials; Glass ionomer; Graphene; Mechanical tests

INTRODUCTION

Among the materials used in minimally invasive dentistry, glass ionomer cements (GICs) have been widely studied since 1970 and are currently recognized as important restorative materials, especially for pediatric dentistry [1,2]. They present a good clinical performance that includes biocompatibility and low cytotoxicity, true adherence to the dental tissues, favorable coefficient of linear thermal expansion, fluoride release, and varied applicability [3-7]. Nevertheless, due to

financial support and Conselho Nacional de Desenvolvimento Científico e Tecnológico (CNPq; 407091/2023).

Conflict of Interest

No potential conflict of interest relevant to this article was reported.

Author Contributions

Conceptualization: Jordão TRS, Silva EJN, Maia LC, Fidalgo TKS; Data curation: Jordão TRS, Fernandes LSV, Alexandria A, Silva EJN, Maia LC, Fidalgo TKS; Formal analysis: Jordão TRS, Fernandes LSV, Leite KLF, Alexandria A, Silva EJN, Maia LC, Fidalgo TKS; Funding acquisition: Fidalgo TKS; Investigation: Jordão TRS, Fernandes LSV, Leite KLF, Alexandria A, Silva EJN, Maia LC, Fidalgo TKS; Methodology: Jordão TRS, Fernandes LSV, Leite KLF, Alexandria A, Silva EJN, Maia LC, Fidalgo TKS; Project administration: Silva EJN, Maia LC, Fidalgo TKS; Resources: Fidalgo TKS; Supervision: Alexandria A, Silva EJN, Maia LC, Fidalgo TKS; Validation: Jordão TRS, Fernandes LSV, Leite KLF, Alexandria A, Silva EJN, Maia LC, Fidalgo TKS; Visualization: Jordão TRS, Fernandes LSV, Leite KLF, Alexandria A, Silva EJN, Maia LC, Fidalgo TKS; Writing - original draft: Jordão TRS, Fernandes LSV, Leite KLF, Alexandria A, Silva EJN, Maia LC, Fidalgo TKS; Writing - review & editing: Jordão TRS, Fernandes LSV, Leite KLF, Alexandria A, Silva EJN, Maia LC, Fidalgo TKS.

ORCID iDs

Tatiane Ramos dos Santos Jordão
https://orcid.org/0000-0001-7143-5050
Laura Soares Viana Fernandes
https://orcid.org/0000-0001-6040-8866
Karla Lorene de França Leite
https://orcid.org/0000-0002-0113-6810
Adílis Alexandria
https://orcid.org/0000-0003-4774-1204
Emmanuel João Nogueira Leal Silva
https://orcid.org/0000-0002-6445-8243
Lucianne Cople Maia
https://orcid.org/0000-0003-1026-9401
Tatiana Kelly da Silva Fidalgo
https://orcid.org/0000-0003-1340-9967

inferior physical-mechanical properties when compared to resin composites, different strategies have been employed over the years to reduce such limitations [8-12]. Some of these strategies included adding silver and tin amalgam alloy powder, incorporating silver nanoparticles, and adding zinc, titanium, barium, and strontium, resin, hydroxyapatite, fibers, zirconium, and other nanometric particles to GICs, which did not improve its properties [13-20].

GICs are widely used materials in dentistry but lack improvements in some properties. Graphene, one of the crystalline forms of carbon, has been identified as a potentially useful material in dentistry, and studies have shown that incorporating graphene into dental materials might improve their performance [21]. Graphene can be obtained through naturally available graphite and appears in the form of nanosheets [22]. Its chemical structure consists of covalently bound carbon atoms (sp^2) in the format of hexagonal rings (honeycombs), where each carbon is bound to 3 other carbons in the structure, which contributes to its unique and versatile material properties [2]. Graphene is considered to be one of the most resistant isolated materials to date, presenting chemical and thermal stability, excellent mechanical properties (resistance to rupture of 42 N/m and Young Module of 1.0 Tpa), high resistance to wear and friction, flexibility, biocompatibility, and antibacterial properties [22-25]. As it presents characteristics compatible with dental materials, graphene stands out for its broad potential for applications in dentistry. Especially when incorporated with restorative materials, such as GIC, graphene, in theory, would make it possible to reduce microfissures in the internal structure, thus protecting the disintegration caused by oral microorganisms [26].

When a new biomaterial for dental applications is produced or modified, it is essential to improve or maintain the physical-mechanical, chemical, and biological properties [27,28]. In this context, graphene addition to GIC could benefit the physical-mechanical parameters. The literature reports improvements in GIC properties when modified by graphene in varied forms, such as oxide, graphene powder, solution or paste; graphene nanoplatelets, and functionalized graphene, which adds elements to its surface. Ghodrati and Sharafeddin [29] demonstrated an increase in shear bond strength when 1% and 2% of graphene were incorporated into self-curing GIC. Chen *et al.* [2] also found a decrease in *Streptococcus mutans* viability after incorporating 1% and 2% graphene-silver nanoparticles into GIC. Thus, the present article sought to evaluate the physical-mechanical, chemical, and biological properties resulting from incorporating graphene at various concentrations (*e.g.*, 0.5%, 1%, 2%, and 5%) into 2 high-viscosity self-curing GICs. The null hypothesis was that adding graphene at different concentrations would not modify the antimicrobial activity, radiopacity, sorption, solubility, microhardness, or fluoride release of GICs.

MATERIALS AND METHODS

Modification of the GICs

Two commercial high-viscosity self-curing GICs were evaluated: Ketac Molar Easy Mix (G_{Ketac}, 3M ESPE, Monrovia, CA, USA) and Fuji IX (G_{Fuji}, GC Corporation, Tokyo, Japan). The

Table 1. Chemical composition of glass ionomers

Material	Composition	Manufacturer
Fuji IX (GC)	Fluoroaluminosilicate glass, multifunctional methacrylate, water, methylmethacrylate, polyacrylic acid, camphorquin	GC Corp, Tokyo, Japan
Ketac Molar Easy Mix (3M ESPE)	Al-Ca-La fluorosilicate glass, ethanediyl ester, copolymer acrylic, maleic acid, and aminoethyl ester dicyclopentyldimethylene diacrylate	3M ESPE AG, Seefeld, Germany

composition of each material is detailed in **Table 1** [30,31].

Graphene powder (carbon nanomaterial, 100% graphene, Lot #MKCL7849, surface area of > 500 m^2/g, Sigma-Aldrich, St. Louis, MO, USA) was mixed into GIC powder at the following concentrations: at the following concentrations: 0.5%, 1%, 2%, and 5% (w/w). To produce the specimens, each cement was divided into 5 groups: (i) no addition of graphene (control group: graphene free), (ii) addition of 0.5% graphene, (iii) addition of 1% graphene, (iv) addition of 2% graphene, and (v) addition of 5% graphene. To maintain the same powder/liquid ratio preconceived by the manufacturer, the same quantity of added graphene powder was removed from GIC powder. The graphene and GIC powders were placed in a transparent plastic tube with a lid and then vigorously manually shaken to obtain a homogeneous mixture without agglomerates and deposits at the bottom of the tube. Prior to sample preparation, the tubes were vigorously manually shaken again according to manufacturer recommendations for GICs.

Condensation silicone matrices (CLONAGE, DFL, Rio de Janeiro, Brazil), with a size of 1.5 mm (height) × 8 mm (diameter) were used to produce the test specimens. The cements of the control group and the experimental specimens were manipulated according to the specifications of each manufacturer. After manipulation, a homogeneous mixture was observed and the materials were inserted into the matrix using a stainless steel spatula and the materials were pressed together with a glass microscopy slide covered with solid petroleum jelly (Vaselina Sólida, Rioquímica, São Paulo, Brazil) [32]. The researchers waited 5 minutes for the materials to be pressed together. All specimens, except those used in the antimicrobial activity tests were stored in a humid medium at 37ºC for 24 hours prior to analysis. The entire process was performed by a single operator. It adopted a sample size of 5 or more for major experiments, based on the ISO 4049 recommendations. Since graphene powder is gray, the visual (macroscopic) analysis of modified GICs was performed for all concentrations (0%, 0.5%, 1%, 2%, and 5% graphene).

Color assessment

The graphene-modified ionomers color was assessed using the Cyan, Magenta, Yellow, and Key mode. The K represents black color and was used to evaluate the samples' colors. It was taken an image of all the specimens together and .tiff file was uploaded in the CorelDRAW Graphics Suite 2024 software (Alludo, Ottawa, Canada). Each specimen was evaluated in 3 different areas obtaining the K scores that represented black percentages. The higher percentages represent more blacks' colors.

Superficial evaluation of the sample by non-contact profilometry

Three specimens were manufactured for each group and concentration of graphene/GIC, totaling 30 samples characterized by 3D non-contact profilometry (Nanovea PS50 Optical, NANOVEA, Irvine, CA, USA). For this, an evaluation of 1 mm^2 on the surface of the specimens was standardized. Three measurements were performed with a confocal chromatic sensor, using a white light axial source, a scanning speed of 2 mm/s, and a refraction rate of 10,000. The averages of the 3 measures of linear roughness (Ra, 500 μm, ISO 4287) and volumetric roughness (Sa, 250 μm^2, ISO 25178) were calculated for each specimen. These analyses were conducted by a single blinded examiner.

Analysis of radiopacity

To conduct this test, 5 discs from each group and each concentration of graphene/GIC were manufactured, totaling 50 samples, measuring 1.5 mm (height) × 8 mm (diameter). Two

primary teeth were used as a standard to visually compare the radiopacity [33]. After the GICs were cured, discs were dispersed onto an occlusal film (IO-41 Occlusal Film, Kodak, Rochester, NY, USA), and a radiograph was taken with an exposure time of 0.65 kV. The radiographic image was digitized and imported into the CorelDRAW Graphics Suite 2017 program (Alludo). A gray intensity scale was generated by the program and used to evaluate the radiopacity of each sample. The gray values were recorded by a single examiner and the average from each group, with their respective graphene concentrations, was calculated.

Analysis of sorption and solubility

The water sorption (W_{Sp}) and solubility (W_{Sl}) tests were conducted based on ISO 4049:2000 standards. The modifications related to disc dimensions were performed according to the literature [34]. Therefore, 4 discs were manufactured, measuring 1.5 mm (height) × 8 mm (diameter) for each group and each concentration of graphene/GIC, totaling 40 samples. Each disc was weighed after 48 hours of manipulation, submerged in 10 mL of distilled water at 37°C and pH 7.0, and weighed again after 24 hours. Subsequently, discs were stored in a desiccator at 37°C and weighed again. The discs were suspended by the nylon filament fixed to the cap to prevent the discs from touching the tube. The process was repeated at intervals of 7, 14, and 21 days. After this period, the water sorption (W_{Sp}) in μg/mm^3 and the solubility of each GIC were calculated. The water sorption [$W_{Sp} = (M_2 - M_3)/V \times 100\%$] and solubility [$S_{Sl} = (M_1 - M_3)/V \times 100\%$] were calculated as percentages of the original mass. Where M_1 is the conditioned mass, in micrograms, prior to immersion in water; M_2 is the mass of the specimen, in micrograms, after immersion in water; M_3 is the mass of the reconditioned specimen, in micrograms; and V is the volume of the specimen, in cubic millimeters.

Vickers microhardness

To conduct this test, 6 discs were manufactured, measuring 1.5 mm (height) × 8 mm (diameter) for each group and each concentration of graphene/GIC, totaling 60 samples. To measure the Vickers microhardness (Buehler, Lake Bluff, IL, USA), a Vickers penetrator was applied to the surface of each sample with a load of 50 g for 10 seconds [35,36]. Measurements were performed in triplicate at equidistant indentations of 100 μm by 1 operator, and the averages for each specimen were calculated.

Antimicrobial activity: inhibition zone test

S. mutans (American Type Culture Collection [ATCC] 25175) was incubated on Brain Heart Infusion (BHI) medium agar in a 20 mL plate at 37°C for 48 hours. Three colonies were isolated and transferred to 20 mL of sterile liquid BHI culture and incubated at 37°C for 24 hours to reach a maximum growth of 1×10^8 colony-forming unit/mL. The bacterial concentration was obtained by measuring the optical density of a 3 mL aliquot and comparing it to the McFarland 0.5 scale.

Twenty-two Petri dishes, containing 10 mL of BHI agar received 2 perforations at equidistant points to create the wells. The perforations were created with a sterile polyester matrix with the dimensions of 4 mm (height) × 3 mm (diameter). The G_{Ketac} and G_{Fuji} GICs of both the control and experimental groups were inserted in the wells before their cure process. For each dish, 2 discs from each group were fixed, totaling 4 discs per group, with a size of 4 mm (height) × 3 mm (diameter). For the positive control, 0.2% chlorhexidine gel (Perioxidin Gel) was inserted into the wells of the 2 plates. After gelation of the GICs, the dishes were sterilized under ultraviolet light for 30 minutes.

https://doi.org/10.5395/rde.2024.49.e37

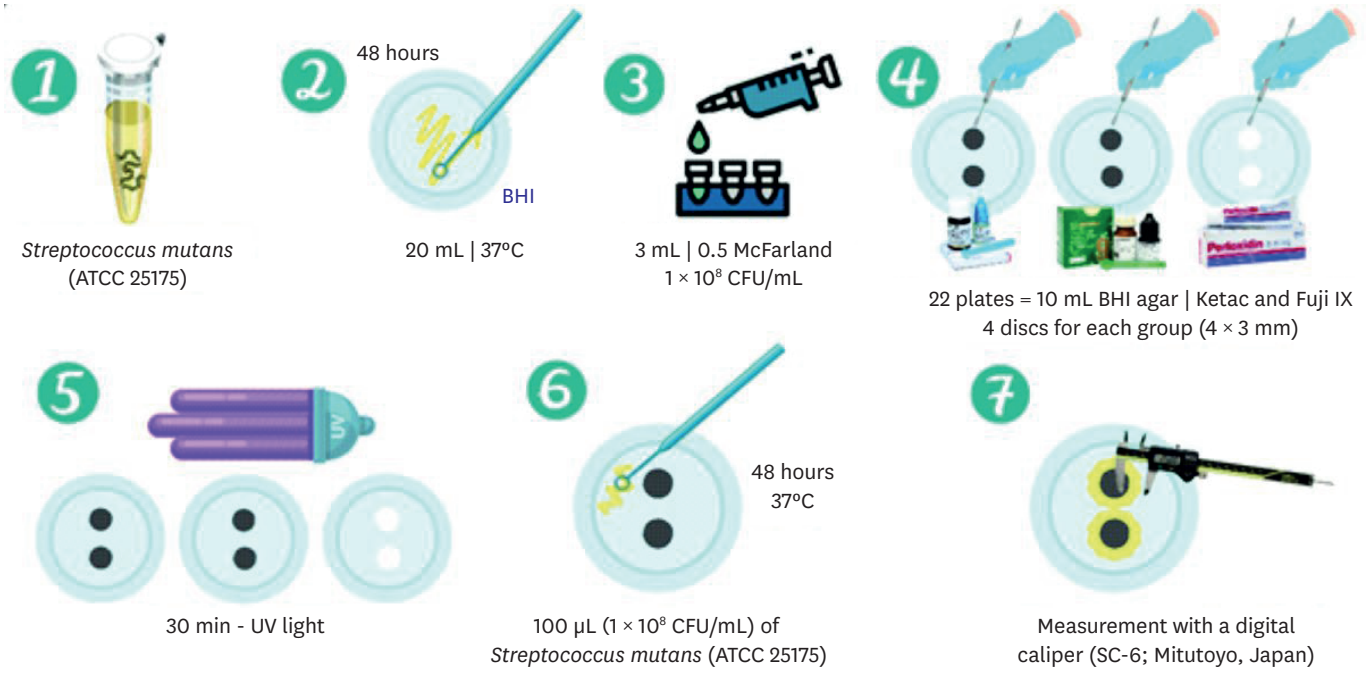

Figure 1. Representative scheme for the zone of inhibition test.
ATCC, American Type Culture Collection; CFU, colony-forming unit; BHI, Brain Heart Infusion; UV, ultraviolet.

A 100 µL (1 × 10⁸ UFC/mL) aliquot of *S. mutans* (ATCC 25175) was spread uniformly on the surface of the culture medium of the 22 dishes, which were then incubated at 37°C for 48 hours. After, the diameters of the inhibition zones around the specimens were measured with a digital pachymeter (SC-6, Mitutoyo, Kawasaki, Japan). Diameters were measured in triplicate, subtracting the disc, and calculating the average and standard deviation for each GIC (**Figure 1**).

Analysis of the fluoride release

To conduct this test, 5 discs were manufactured, measuring 1.5 mm (height) × 8 mm (diameter) for each group and each concentration of graphene/GIC, totaling 50 samples. Discs were stored in relative humidity for 24 hours at 37°C. Afterward, they were immersed in 10 mL of deionized water for 24 hours, and 7, 14, 21, and 28 consecutive days after their manufacture, changing the solution between each period. The discs were suspended by a nylon filament fixed to the cap to prevent the discs from touching the tube. Scanning for fluoride in 1 mL of the sample was performed in duplicate with a selective electrode (Orion, São Paulo, Brazil). Prior to the readings, calibrations were conducted with sodium fluoride solutions of 0.125–0.500 ppm, prepared with total ionic strength adjustment buffer II in a 1:1 proportion.

Data analysis

Data were tabulated and analyzed with SPSS 20.0 statistics program (SPSS Inc, Chicago, IL, USA). The Shapiro-Wilk test was used to test the normality of the data and determine the appropriate statistical tests. Profilometry (Ra and Sa), solubility, sorption, and fluoride release presented non-normal distributions and were, therefore, evaluated using the Kruskal-Wallis and Mann-Whitney tests for unpaired independent data when assessing the different groups and the Wilcoxon test for dependent data when assessing the same sample over time. Radiopacity and microhardness presented normal distributions and were, therefore, evaluated with a 1-way analysis of variance and Tukey's test. The main objective of graphene incorporation was to improve the mechanical resistance; therefore, the power analysis was

assessed based on microhardness, by comparing 0% and 5% incorporation for G_{Fuji} and G_{Ketac}. A 95% confidence interval was adopted for all tests ($p \leq 0.05$).

RESULTS

The power analysis comparing 0% and 5% graphene incorporation into G_{Fuji} and G_{Ketac} demonstrated a power of 100% and 34.82%, respectively.

Color assessment

The percentages of K (black) for G_{Ketac} from 0% to 5% were: 27%, 69%, 79%, 89%, and 89%. The percentages for G_{Fuji} from 0% to 5% were: 25%, 83%, 91%, 95%, and 99%. A visual assessment and color analysis using the images demonstrated that after adding graphene, the ionomers turned gray. The shades of gray were proportional to the graphene concentration. Higher concentrations of graphene powder (5%) resulted in a darker gray sample compared to lower concentrations (0.5%; **Figure 2**).

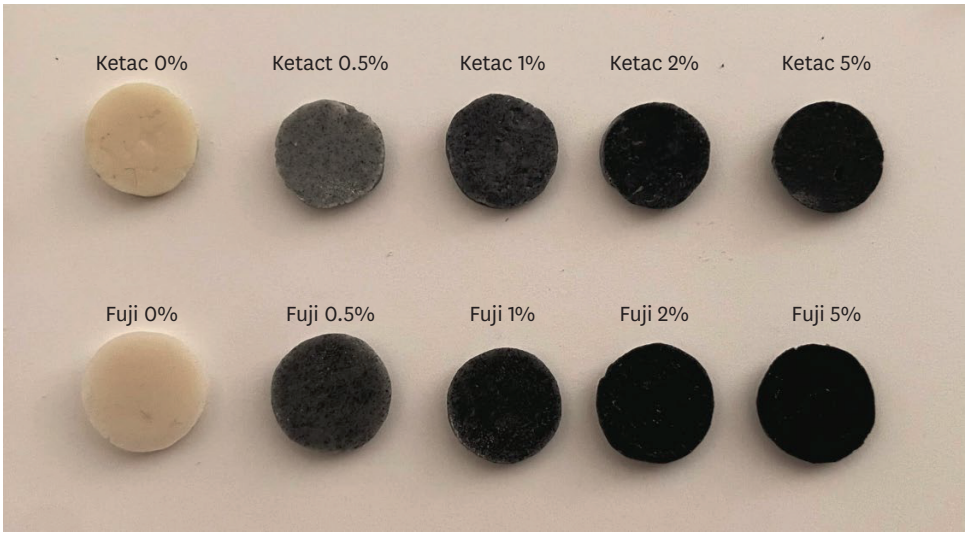

Figure 2. Image representative demonstrating the color change after graphene incorporation.

Table 2. Means and 95% confident intervals (CIs) for the means of linear roughness (Ra) and volumetric roughness (Sa) values

Material	Group	Profilometry			
		Ra		Sa	
		Mean (CI)	Statistical difference	Mean (CI)	Statistical difference
Ketac	G_{Ketac} 0%^{A}	4.05 (3.87–4.35)	AB, AC	4.76 (3.42–8.78)	AB, AC, AE, **AF**
	G_{Ketac} 0.5%^{B}	1.90 (1.10–1.98)	BA, BC, BD, BE	2.07 (1.31–2.14)	BA, BD, BE
	G_{Ketac} 1%^{C}	2.64 (1.85–3.11)	CA, CB, CE, **CH**	2.40 (2.19–3.22)	CA
	G_{Ketac} 2%^{D}	3.31 (2.14–4.56)	DB	4.09 (2.20–4.71)	DB, **DI**
	G_{Ketac} 5%^{E}	3.40 (2.79–3.47)	EB, EC, **EJ**	4.05 (3.80–4.52)	AE, EB, **EJ**
Fuji	G_{Fuji} 0%^{F}	2.72 (2.17–3.62)	FG, FH, FI, FJ	5.16 (4.87–5.37)	FH, FI, FJ, **FA**
	G_{Fuji} 0.5%^{G}	1.84 (1.45–2.25)	GF	2.57 (1.55–3.41)	-
	G_{Fuji} 1%^{H}	1.71 (1.33–2.07)	HF, HI, HJ, **HC**	1.88 (1.87–1.95)	HF
	G_{Fuji} 2%^{I}	1.55 (1.42–2.04)	IF, IH	2.82 (2.80–4.36)	IF, **ID**
	G_{Fuji} 5%^{J}	1.90 (1.64–1.98)	JF, JH, **JE**	2.71 (2.42–2.88)	JF, **JE**

Kruskal-Wallis and Mann-Whitney test ($p \leq 0.05$).
Capital letters indicate the different groups. The 2 letters represent the statistic difference between groups: plain letters indicate statistical differences in concentration considering the same GIC and bold letters indicates statistical differences considering the same graphene concentration, but comparing G_{Ketac} and G_{Fuji}.

https://doi.org/10.5395/rde.2024.49.e37

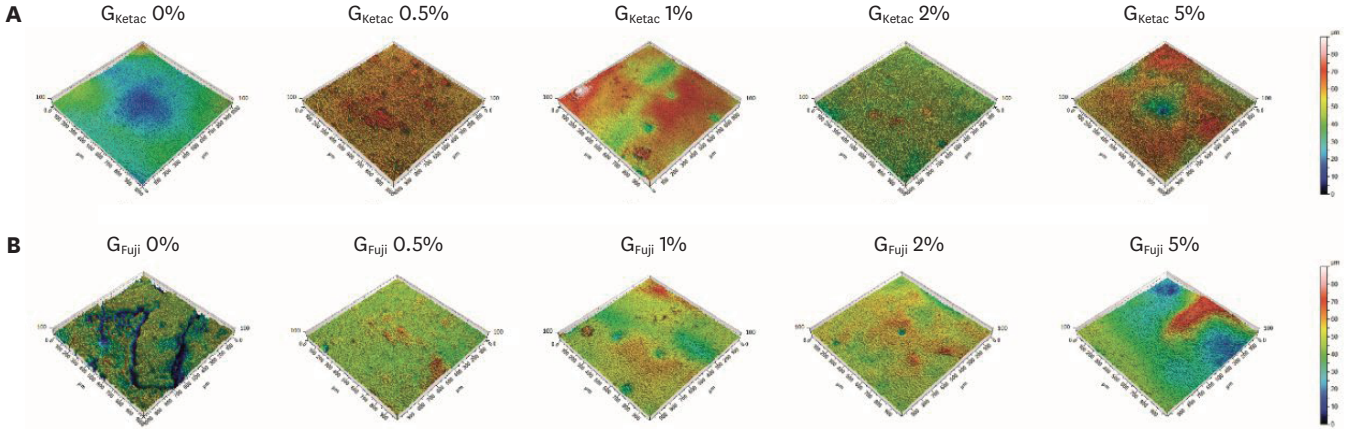

Figure 3. Representative images showing the superficial surface (1 mm²) of (A) G_{Ketac} discs, and (B) G_{Fiji} discs. The color scale indicates the variation in micrometers varying from 0 µm (blue) to 100 µm (red).

Analysis of surface topography

The Ra and Sa values, as well as the mean and standard deviation, are presented in **Table 2**. Statistical analysis showed Ra was significantly higher in G_{Ketac} 0% and G_{Fuji} 0% compared to the other concentrations ($p \leq 0.05$). Sa also presented higher values for G_{Ketac} 0% when compared to G_{Ketac} 0.5%, 1%, and 5%; for $G_{Fuji,}$ the 0% presented higher Sa than 1%, 2%, and 5% ($p \leq 0.05$). **Figure 3** shows the samples of G_{Ketac} and G_{Fuji}. G_{Ketac} 0% and 5% presented higher superficial irregularity, as did G_{Fuji} 0% and 0.5%.

Analysis of radiopacity

According to the grayscale and with average values obtained for each group for G_{Ketac} and G_{Fuji}, the radiopacity was significantly lower in G_{Fuji} 5% ($p \leq 0.05$; **Table 3**). For G_{Ketac} 0% and the other concentrations of $G_{Fuji,}$ there were no statistically significant differences in the radiopacity of the samples ($p > 0.05$). In the comparison between G_{Ketac} and G_{Fuji}, this last 1 presented higher radiopacity values for 0% and 1%.

Analysis of solubility and water sorption

The results for solubility and water sorption are detailed in **Tables 4** and **5**, respectively. Comparing G_{Ketac} and G_{Fuji} at the same concentration and time point, the data showed lower solubility for G_{Fuji} 0% and G_{Fuji} 5% at 24 hours and 14 days ($p \leq 0.05$). The sorption was lower

Table 3. Average values of gray and standard deviation (SD) obtained for each sample and their respective concentrations of ionomer/graphene

	Groups	Mean ± SD	Statistical difference
Ketac	G_{Ketac} 0%^{A}	49.00 ± 4.76	**AF**
	G_{Ketac} 0.5%^{B}	49.00 ± 2.58	-
	G_{Ketac} 1%^{C}	48.25 ± 2.75	**CH**
	G_{Ketac} 2%^{D}	45.75 ± 8.22	-
	G_{Ketac} 5%^{E}	45.50 ± 2.38	-
Fuji	G_{Fuji} 0%^{F}	64.25 ± 2.22	FJ, **FA**
	G_{Fuji} 0.5%^{G}	64.00 ± 1.41	GJ
	G_{Fuji} 1%^{H}	63.00 ± 7.87	HJ, **CH**
	G_{Fuji} 2%^{I}	56.75 ± 7.93	-
	G_{Fuji} 5%^{J}	47.75 ± 6.02	JF, JG, JH

One-way analysis of variance and Tukey's test ($p \leq 0.05$).
Capital letters indicate the different groups. The 2 letters represent the statistical difference between groups: plain letters indicate statistical differences in concentration considering the same GIC and bold letters indicate statistical differences considering the same graphene concentration, but comparing G_{Ketac} and G_{Fuji}.

https://doi.org/10.5395/rde.2024.49.e37

Table 4. Means and 95% confident intervals (CIs) for the means of the solubility (%S) tests of the samples after 24 hours, and 7, 14, and 21 days

Groups	Solubility (%S)				
	24 hr	7 d	14 d	21 d	Statistical difference
G_{Ketac} 0%^{A}	3.79 (3.50–4.13)	3.61 (3.43–3.79)	3.20 (3.00–3.44)	3.04 (2.61–3.32)	AB_{7d}, AD_{7d}, **AF_{24hr}**, **AF_{7d}**, **AF_{14d}**, **AF_{21d}**
G_{Ketac} 0.5%^{B}	4.02 (3.65–4.25)	3.99 (3.91–4.04)	3.59 (3.19–3.61)	3.40 (3.33–6.06)	BA_{7d}, BC_{7d}, BD_{7d}
G_{Ketac} 1%^{C}	3.83 (3.59–4.24)	3.63 (3.17–3.81)	3.34 (3.10–3.67)	3.10 (2.64–3.38)	CB_{7d}, **CH_{7d}**
G_{Ketac} 2%^{D}	3.87 (3.57–4.00)	3.09 (2.89–3.37)	2.74 (2.59–3.07)	2.91 (2.66–3.13)	DA_{7d}, DB_{7d}, **DI_{7d}**
G_{Ketac} 5%^{E}	4.05 (3.48–4.33)	3.44 (2.67–4.04)	3.25 (2.67–3.79)	3.39 (2.90–3.81)	**EJ_{24hr}**, **EJ_{14d}**
G_{Fuji} 0%^{F}	2.40 (1.94–2.85)	2.23 (1.32–2.37)	1.94 (1.57–2.41)	1.81 (1.32–2.04)	**FA_{24hr}**, **FA_{7d}**, **FA_{14d}**, **FA_{21d}**
G_{Fuji} 0.5%^{G}	10.20 (0.14–16.32)	10.77 (0.14–16.45)	10.25 (0.92–16.05)	10.08 (0.85–15.91)	-
G_{Fuji} 1%^{H}	3.62 (2.77–3.93)	1.95 (1.36–2.59)	2.59 (2.40–11.86)	8.85 (1.68–16.19)	**HC_{7d}**
G_{Fuji} 2%^{I}	3.93 (3.29–4.29)	3.98 (3.44–4.39)	3.19 (2.45–3.92)	3.30 (2.22–3.72)	**ID_{7d}**
G_{Fuji} 5%^{J}	0.59 (0.51–3.78)	1.76 (0.51–4.32)	0.74 (0.58–2.90)	0.07 (0.00–3.11)	**JE_{24hr}**, **JEb_{14d}**

Kruskal-Wallis and Mann-Whitney test ($p \leq 0.05$): comparisons of different concentrations between glass ionomer cements (GICs) and different concentrations in the same GIC group. Wilcoxon test ($p \leq 0.05$): comparisons of difference the period of times in the same GIC group.
Capital letters indicate the different groups. The 2 letters represent the statistic difference between groups: plain letters indicate statistical differences in concentration considering the same GIC and bold letters indicate statistical differences considering the same graphene concentration but comparing G_{Ketac} and G_{Fuji}. The subscript letters indicate the periods.

Table 5. Means and 95% confident intervals (CIs) for the means of water sorption (%WS) after 24 hours, and 7, 14, and 21 days

Groups	Water sorption (%WS)				
	24 hr	7 d	14 d	21 d	Statistical difference
G_{Ketac} 0%^{A}	3.71 (3.41–4.02)	3.53 (3.26–3.70)	3.15 (2.96–3.38)	2.95 (2.61–3.27)	AB_{7d}, AC_{7d} AB_{21d}, **AF_{24hr}**, **AF_{7d}**, **AF_{14d}**, **AF_{21d}**
G_{Ketac} 0.5%^{B}	3.89 (3.52–4.12)	3.93 (3.87–3.96)	3.52 (3.15–3.55)	3.36 (3.31–5.97)	BA_{7d}, BC_{7d}, BD_{7d}, BE_{7d}, BD_{14d}, BA_{21d} BD_{21d}
G_{Ketac} 1%^{C}	3.65 (3.42–4.12)	3.54 (3.12–3.73)	3.28 (2.95–3.59)	3.06 (2.60–3.37)	$CA_{7d,}$ CB_{7d}, CD_{7d}, $CD_{14d,}$ **CI_{7d}**
G_{Ketac} 2%^{D}	3.71 (3.49–3.83)	2.96 (2.67–3.21)	2.67 (2.53–3.00)	2.86 (2.62–3.10)	DB_{7d}, DC_{7d}, DB_{14d}, DC_{14d} DB_{21d}
G_{Ketac} 5%^{E}	3.88 (3.34–4.21)	3.25 (2.56–3.90)	3.14 (2.57–3.65)	3.28 (2.79–3.74)	EB_{7d}, **EJ_{24hr}**, **EJ_{14d}**
G_{Fuji} 0%^{F}	2.38 (1.91–2.83)	2.18 (1.28–2.32)	1.90 (1.52–2.35)	1.76 (1.28–1.99)	**FA_{24hr}**, **FA_{7d}**, **FA_{14d}**, **FA_{21d}**
G_{Fuji} 0.5%^{G}	10.54 (0.14–18.29)	10.58 (0.14–18.00)	10.75 (0.85–17.56)	10.49 (0.78–17.24)	-
G_{Fuji} 1%^{H}	3.59 (2.75–3.90)	1.90 (1.33–2.55)	3.96 (2.35–11.60)	8.65 (1.63–15.75)	-
G_{Fuji} 2%^{I}	3.89 (3.25–4.23)	3.83 (3.26–4.26)	3.13 (2.37–3.83)	3.21 (2.15–3.62)	**IC_{7d}**
G_{Fuji} 5%^{J}	0.57 (0.48–3.77)	1.73 (0.47–4.08)	0.76 (0.55–2.83)	0.07 (0.00–3.05)	**JE_{24hr}**, **JE_{14d}**

Kruskal-Wallis and Mann-Whitney test ($p \leq 0.05$): comparisons of different concentrations between glass ionomer cements (GICs) and different concentration in the same GIC group. Wilcoxon test ($p \leq 0.05$): comparisons of difference the period of times in the same GIC group.
Capital letters indicate the different groups. The 2 letters represent the statistic difference between groups: plain letters indicate statistical differences in concentration considering the same GIC and bold letters indicate statistical differences considering the same graphene concentration but comparing G_{Ketac} and G_{Fuji}. The subscript letters indicate the periods.

in G_{Fuji} 0% compared to G_{Ketac} 0% at all periods of time and G_{Fuji} 5% also presented lower sorption compared to G_{Ketac} 5% at 24hours and 14 days ($p \leq 0.05$).

Regarding the comparisons of the time points, considering the same GIC group and graphene concentration, the data showed no difference in solubility and sorption for G_{Ketac} and G_{Fuji} ($p > 0.05$).

For solubility, regarding the comparisons related to the different graphene concentrations, considering the same group and time point, higher solubility was observed in G_{Ketac} 0.5% compared to 0%, 1%, and 2% at 7 days ($p \leq 0.05$). There were no differences observed between the different concentrations for G_{Fuji} ($p > 0.05$). For water sorption, higher solubility was observed in G_{Ketac} 0.5% compared to 0%, 1%, and 5% at 14 days ($p \leq 0.05$).

Vickers microhardness

The Vickers microhardness test (**Table 6**) did not indicate any changes in the microhardness of the same GIC at different concentrations of graphene, except for G_{Fuji} 0%, which showed a significant reduction in its microhardness compared to G_{Fuji} 5% ($p = 0.001$).

https://doi.org/10.5395/rde.2024.49.e37

Table 6. Analysis of the average and standard deviation (SD) of the samples in the Vickers microhardness trial.

Materials	Groups	Mean ± SD	Statistical difference
Ketac	G_{Ketac} 0%^{A}	59.23 ± 7.24	AF
	G_{Ketac} 0.5%^{B}	62.01 ± 14.57	-
	G_{Ketac} 1%^{C}	65.28 ± 11.56	-
	G_{Ketac} 2%^{D}	59.66 ± 15.23	-
	G_{Ketac} 5%^{E}	52.31 ± 6.69	-
Fuji	G_{Fuji} 0%^{F}	79.17 ± 5.76	FA, FJ
	G_{Fuji} 0.5%^{G}	67.55 ± 3.66	-
	G_{Fuji} 1%^{H}	68.41 ± 5.25	-
	G_{Fuji} 2%^{I}	62.70 ± 10.15	-
	G_{Fuji} 5%^{J}	53.03 ± 5.32	-

One way analysis of variance and Tukey's test; $p \leq 0.05$.
Capital letters indicate the different groups. The 2 letters represent the statistic difference between groups.

Antimicrobial activity

There was no evidence of antimicrobial activity against *S. mutans* when the different samples from the control (graphene-free) and experimental (0.5%, 1%, 2%, and 5%) groups of G_{Ketac} and G_{Fuji} were evaluated. A zone of inhibition was only observed in the positive control with the 0.2% chlorhexidine (Perioxidin Gel) of 7.54 ± 0.63 mm.

Analysis of fluoride release

Figure 4 shows the fluoride release profiles. Considering the days and the comparisons within groups (different concentrations of the same material), no statistical differences were observed between 24 hours and 7 days for the concentrations 0% and 0.5%, for G_{Ketac} and G_{Fuji} ($p > 0.05$). After 14 days G_{Ketac} 2% and 5% released more fluoride than 0%, 0.5%, and 1%. After 14 days, G_{Fuji} released more fluoride for 0% and 5% ($p \leq 0.05$). After 21 days, G_{Ketac} 5%, 2%,

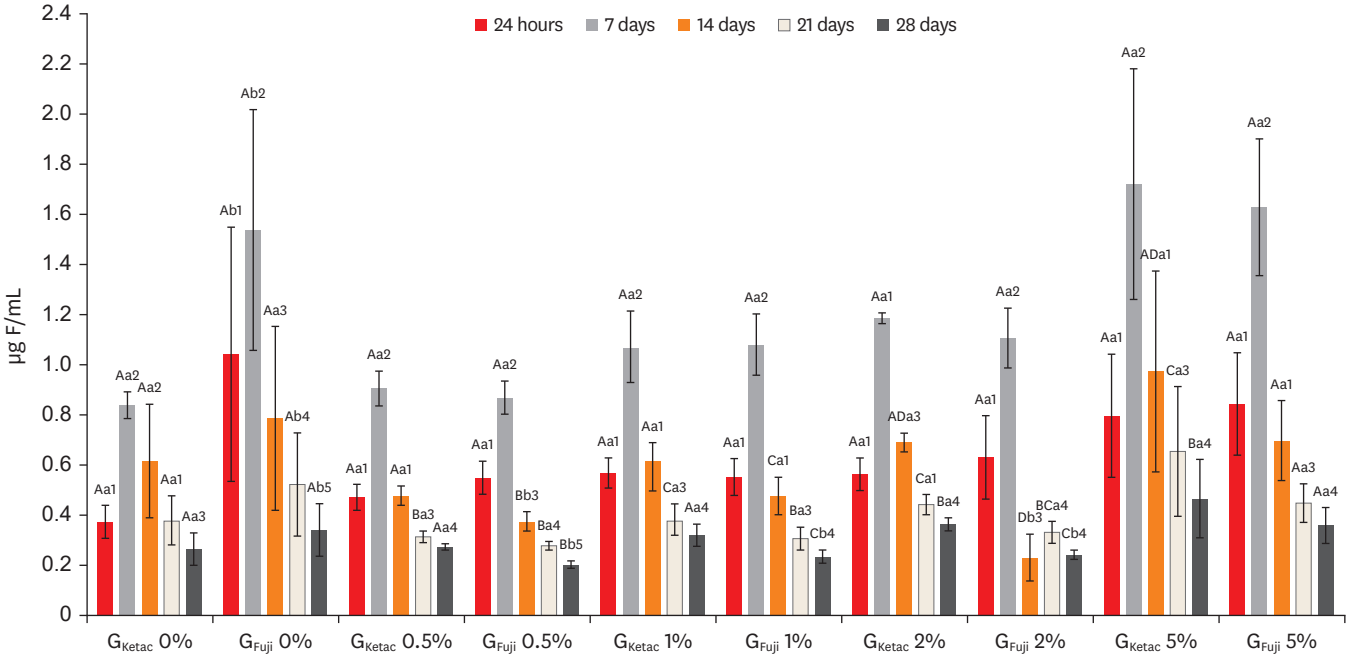

Figure 4. G_{Ketac} and G_{Fuji} fluoride release (0%, 0.5%, 1%, 2%, and 5%) after 24 hours, and 7, 14, 21, and 28 days.
Different capital letters indicate statistically significant differences within the groups (considering the different time points and the different concentrations of the same glass ionomer cement [GIC]); different small letters indicate statistically significant differences between the groups (considering the same time points and graphene concentration between G_{Ketac} and G_{Fuji}); and different numbers indicate significant differences when comparing the same materials in the different time points (considering the periods of release in the same GIC and graphene concentration).

https://doi.org/10.5395/rde.2024.49.e37

and 1% released more fluoride than 0% and 0.5% ($p \leq 0.05$). In the same period, G_{Fuji} released more fluoride for 0% and 5% ($p \leq 0.05$). After 28 days, G_{Ketac} released similar levels of fluoride for all concentrations, and G_{Fuji} presented lower fluoride release for all groups, except for 5%.

Comparing between groups (considering the same time point and graphene concentration among G_{Ketac} and G_{Fuji}), after 24 hours and 7 days, G_{Ketac} 0% and 0.5% exhibited lower fluoride release than $G_{Fuji.}$0% and 0.5%, respectively ($p \leq 0.05$). After 14 days, similar levels of fluoride were released for G_{Ketac} and $G_{Fuji,}$ for all graphene concentrations ($p > 0.05$). After 21 days, G_{Fuji} 0% released more fluoride than G_{Ketac} 0% ($p > 0.05$). After 28 days, G_{Fiji} released higher levels of fluoride in 0% than $G_{Ketac.}$ G_{Ketac} released higher levels of fluoride at 0.5%, 1%, and 2% compared to the same concentrations for G_{Fiji}.

Regarding the time points (considering the periods of release in the same GIC and graphene concentration), greater fluoride release was observed at 7 days for most of the groups, showing a drop after 14 and 21 days. After 24 hours, the highest concentration of fluoride was present in both materials, with a progressive reduction in fluoride released after 14, 21, and 28 days, except for G_{Fuji} 2%.

DISCUSSION

Recent studies with nanomaterials made of graphene established antibacterial activity against *S. mutans*, which depends on the physical size of the structure and the number of nanosheet layers [22,24,25,37-40]. One of the theories is that the laminated structures penetrate the membrane of the bacterial cells more easily using physical force (van der Waals force), rupturing them and causing their cell death, but it is still not fully understood how graphene and its derivatives can cause the antimicrobial activity [41,42]. Contrary to these findings, the present study did not identify antimicrobial activity in the analyzed specimens. We used the inhibition zone test because it is a classical test that is easily conducted; however, it is important to highlight that the diffusion capability of graphene and GIC components could indicate a false negative result for antibacterial activity in this test. Therefore, these results must be interpreted with caution.

Additional investigations using different antibacterial activity methodologies should be performed to determine whether graphene inhibits *S. mutans*. Moreover, one plausible reason for the different results could be the form of graphene used. The mentioned above did not use graphene powder, as the present study, but instead and in most cases, used graphene oxide and other derivatives. In a way, the absence of antimicrobial potential would not preclude the use of the material, since dental caries are a sugar-dependent biofilm with disease resulting from a dysbiotic biofilm [43].

The literature reinforces the importance of radiopacity in restorative materials, which helps the dentist evaluate the integrity of the restoration, verify flaws and protrusions, detect empty spaces and suitable shapes, or even the locate misplaced fragments in the case of traumatic accidents or surgical procedures [44]. According to the American Dental Association's recommendations, radiopacity corresponding to 1-mm-thick materials should at least be equal to 1-mm-thick pure Al, which is also equivalent to 1-mm-thick dentin tissue [45,46]. The ideal is that the restorative materials present radiopacity similar to or higher than enamel for better dental caries identification [47,48]. The components responsible for conferring radiopacity are silver alloy, zinc, strontium, and barium, and this property depends on its

concentration [49]. It is important to highlight that the samples were 1.5 mm thick and that radiopacity may vary according to the thickness of the material used [50]. In the present study, graphene diminished radiopacity at G_{Fuji} 5%, yet the material was still visible and easily identified in radiographic images. For future studies, the adjustment of thicknesses should be considered for obtaining a material with the ideal radiopacity that allows its identification without impairing the visualization of possible demineralization surrounding dental tissue.

GICs are hypersensitive to humidity, since, due to the hydrolysis of the cement matrix, water sorption leads to degradation over time and to the loss of surface properties, edge integrity, esthetic appearance, and, consequently, an increase in the deterioration of restorations [51]. The process of water sorption can be explained by 2 theories. One is that the water molecules spread in micropores and interact with the material's matrix. The other proposes that the water molecules connect to the hydrophilic cement groups, resulting in expansion and an increase in weight [52]. The GIC presents a hydrophilic character and suffers frequent water sorption. Therefore, in a clinical routine, it is important that the GIC restoration be immediately protected by solid petroleum jelly, varnish, or a low-viscosity adhesive [7]. The present study did not use a coat to better assess the water sorption and solubility of modified GICs. The solubility is also an important aspect to monitor, since, upon contact with oral fluids, the GICs can be dissolved gradually, especially in the first 24 hours of environmental pressure. The high solubility and initial syneresis can result in a dimensional change, the formation of pores, and reduced mechanical properties [53]. The present study demonstrated lower sorption and solubility for G_{Fuji} 0% compared to G_{Ketac} 0% in all time points assessed. Incorporating 5% of graphene in both GICs reduced solubility and sorption in 14 days. It is suggested that the graphene powder could make the water flow through GIC polymers. This reduction of sorption and solubility is beneficial to avoid GIC deterioration [51].

The restorative materials should present sufficient hardness to be resistant to masticatory forces. Previous studies concluded that the addition of graphene derivatives in GIC improved its mechanical properties, including hardness [6,54]. However, in the present study, incorporating graphene decreased the microhardness of G_{Fuji} by 5%. This likely resulted from the form of graphene that was used, specifically, the shape, size, and amount of graphene particles used (graphene powder). Another study demonstrated that carbon-based materials can cluster around the matrix [55]. It is suggested that there was no homogeneous dispersion of graphene particles over the GIC matrix, generating an agglomerate, which hinders matrix hydration and forms voids, or zones of weakness of the modified material, resulting in a lower hardness.

It is well documented in the literature that fluoride release from GICs can occur over a long period of time with the potential for reabsorbing the fluoride, thereby promoting an anticaries benefit [56-58]. In an assertive manner, the results of the present study indicate that the incorporation of graphene increased fluoride release for G_{Ketac} and G_{Fuji} with a dose-dependent effect; that is, the greater the concentration of graphene in the sample, the greater the amount of fluoride released. Our results demonstrated a peak in fluoride released for most samples at 7 days. The greater fluoride release during this period possibly occurred because, although a greater release was expected in the initial period of 24 hours, the time was still less than the accumulation of the subsequent period, which was 7 days. The presence of fluoride in the oral cavity, particularly in a biofilm on the tooth surface, can act to minimize demineralization and activate remineralization, resulting in a decrease in the progression of mineral loss. Despite this concept, the notion that fluoride released around the restoration

may play a supporting role in the dental caries process is controversial, especially because there is limited clinical information [59,60]. The possibility of fluoride in a modified GIC matrix deserves attention in further graphene studies.

A limitation of the present study was the manual shaking to homogenize graphene particles and GIC powder. Although the color assessment of GICs was preliminary, the color change of GIC incorporated with graphene can be pointed out as a limitation since aesthetically unfavorable, therefore is suggested that this material could be used as a cavity liner. Otherwise, this is a preliminary study and in future further studies, the color change must be validated with an adequate methodology. If the present findings are confirmed, it will be necessary to treat this modified GIC to improve color or test lower graphene concentrations. Although the sample size was based on ISO 4049 recommendations, which recommends 5 samples per group, the power analysis of microhardness results demonstrated a power of 100% and 34.82% for comparisons of 0% and 5% incorporation for G_{Fuji} and G_{Ketac}, respectively. If the sample size were higher, the power analysis would be improved and would likely result in statistically significant differences in microhardness. Finally, there is a limitation related to the *in vitro* experiments that were conducted in a controlled laboratory environment, making it impossible to reconstruct the real features of the oral cavity.

For a new dental material to be consolidated on the market, numerous tests must be performed. This *in vitro* study was of paramount importance and the first step to better elucidate the behavior of GICs reinforced with graphene and ensure the safety of its use for future incorporation into clinical trials. Among the limitations of the present study, the grayish coloration after reinforcement with graphene must be assessed with caution. This material should be studied more in depth to evaluate its acceptability in restorations and in that which concerns possible modifications so that the coloration becomes more similar to the color of the dental substrate.

CONCLUSIONS

Taking these findings into account, one can suggest that, considering the limitations of the present study, the incorporation of graphene into GICs in lower concentrations (0.5% and 1%) presented only good perspectives for microhardness properties, however, the other properties must be observed with caution since it did not result in a real benefit. Therefore, the null hypothesis was accepted for antimicrobial activity, radiopacity, sorption, solubility, and fluoride release and rejected for microhardness. In addition, considering the above-mentioned limitation. It is important to highlight that the experiments were conducted in a controlled laboratory environment and that it would be impossible to reconstruct the real features of the oral cavity. Further research should be carried out to delimit the properties of graphene-modified GICs.

ACKNOWLEDGEMENTS

This study is part of Jordão TRS masters' thesis at Dental School of Universidade do Estado do Rio de Janeiro (UERJ).

REFERENCES

1. McLean JW, Wilson AD. The clinical development of the glass-ionomer cements. I. Formulations and properties. Aust Dent J 1977;22:31-36. PUBMED | CROSSREF
2. Chen J, Zhao Q, Peng J, Yang X, Yu D, Zhao W. Antibacterial and mechanical properties of reduced graphene-silver nanoparticle nanocomposite modified glass ionomer cements. J Dent 2020;96:103332. PUBMED | CROSSREF
3. Wiegand A, Buchalla W, Attin T. Review on fluoride-releasing restorative materials--fluoride release and uptake characteristics, antibacterial activity and influence on caries formation. Dent Mater 2007;23:343-362. PUBMED | CROSSREF
4. Lan WH, Lan WC, Wang TM, Lee YL, Tseng WY, Lin CP, *et al.* Cytotoxicity of conventional and modified glass ionomer cements. Oper Dent 2003;28:251-359. PUBMED
5. Hume WR, Mount GJ. *In vitro* studies on the potential for pulpal cytotoxicity of glass-ionomer cements. J Dent Res 1988;67:915-918. PUBMED | CROSSREF
6. Sun L, Yan Z, Duan Y, Zhang J, Liu B. Improvement of the mechanical, tribological and antibacterial properties of glass ionomer cements by fluorinated graphene. Dent Mater 2018;34:e115-e127. PUBMED | CROSSREF
7. Sidhu SK, Nicholson JW. A review of glass-ionomer cements for clinical dentistry. J Funct Biomater 2016;7:16. PUBMED | CROSSREF
8. Paiva L, Fidalgo TKS, da Costa LP, Maia LC, Balan L, Anselme K, *et al.* Antibacterial properties and compressive strength of new one-step preparation silver nanoparticles in glass ionomer cements (NanoAg-GIC). J Dent 2018;69:102-109. PUBMED | CROSSREF
9. Al-Angari SS, Hara AT, Chu TM, Platt J, Eckert G, Cook NB. Physicomechanical properties of a zinc-reinforced glass ionomer restorative material. J Oral Sci 2014;56:11-16. PUBMED | CROSSREF
10. Silva RM, Pereira FV, Mota FA, Watanabe E, Soares SM, Santos MH. Dental glass ionomer cement reinforced by cellulose microfibers and cellulose nanocrystals. Mater Sci Eng C 2016;58:389-395. PUBMED | CROSSREF
11. Tiwari S, Kenchappa M, Bhayya D, Gupta S, Saxena S, Satyarth S, *et al.* Antibacterial activity and fluoride release of glass-ionomer cement, compomer and zirconia reinforced glass-ionomer cement. J Clin Diagn Res 2016;10:ZC90-ZC93. PUBMED | CROSSREF
12. Wang Y, Darvell BW. Hertzian load-bearing capacity of a ceramic-reinforced glass ionomer cement stored wet and dry. Dent Mater 2009;25:952-955. PUBMED | CROSSREF
13. Simmons JJ. The miracle mixture. Glass ionomer and alloy powder. Tex Dent J 1983;100:6-12. PUBMED
14. Paiva LF, Fidalgo TK, Maia LC. Mineral content of ionomer cements and preventive effect of these cements against white spot lesions around restorations. Braz Oral Res 2014;28:1-9. PUBMED | CROSSREF
15. Ching HS, Luddin N, Kannan TP, Ab Rahman I, Abdul Ghani NR. Modification of glass ionomer cements on their physical-mechanical and antimicrobial properties. J Esthet Restor Dent 2018;30:557-571. PUBMED | CROSSREF
16. Mitra SB. Adhesion to dentin and physical properties of a light-cured glass-ionomer liner/base. J Dent Res 1991;70:72-74. PUBMED | CROSSREF
17. Lucas ME, Arita K, Nishino M. Toughness, bonding and fluoride-release properties of hydroxyapatite-added glass ionomer cement. Biomaterials 2003;24:3787-3794. PUBMED | CROSSREF
18. Garoushi S, Vallittu P, Lassila L. Hollow glass fibers in reinforcing glass ionomer cements. Dent Mater 2017;33:e86-e93. PUBMED | CROSSREF
19. Gu YW, Yap AU, Cheang P, Koh YL, Khor KA. Development of zirconia-glass ionomer cement composites. J Non-Cryst Solids 2005;351:508-514. CROSSREF
20. Najeeb S, Khurshid Z, Zafar MS, Khan AS, Zohaib S, Martí JM, *et al.* Modifications in glass ionomer cements: nano-sized fillers and bioactive nanoceramics. Int J Mol Sci 2016;17:1134. PUBMED | CROSSREF
21. Novoselov KS, Fal'ko VI, Colombo L, Gellert PR, Schwab MG, Kim K. A roadmap for graphene. Nature 2012;490:192-200. PUBMED | CROSSREF
22. Syama S, Mohanan PV. Safety and biocompatibility of graphene: a new generation nanomaterial for biomedical application. Int J Biol Macromol 2016;86:546-555. PUBMED | CROSSREF
23. Lee C, Wei X, Kysar JW, Hone J. Measurement of the elastic properties and intrinsic strength of monolayer graphene. Science 2008;321:385-388. PUBMED | CROSSREF
24. Tu Y, Lv M, Xiu P, Huynh T, Zhang M, Castelli M, *et al.* Destructive extraction of phospholipids from *Escherichia coli* membranes by graphene nanosheets. Nat Nanotechnol 2013;8:594-601. PUBMED | CROSSREF

25. Al-Jumaili A, Alancherry S, Bazaka K, Jacob MV. Review on the antimicrobial properties of carbon nanostructures. Materials (Basel) 2017;10:1066. PUBMED | CROSSREF
26. Sarosi C, Biris AR, Antoniac A, Boboia S, Alb C, Antoniac I, *et al*. The nanofiller effect on properties of experimental graphene dental nanocomposites. J Adhes Sci Technol 2016;30:1779-1794. CROSSREF
27. Yadav R, Meena A, Patnaik A. Biomaterials for dental composite applications: a comprehensive review of physical, chemical, mechanical, thermal, tribological, and biological properties. Polym Advan Technol 2022;33:1762-1781. CROSSREF
28. Tiu J, Belli R, Lohbauer U. A step toward bio-inspired dental composites. Biomater Investig Dent 2023;10:2150625. PUBMED | CROSSREF
29. Ghodrati P, Sharafeddin F. Evaluation of the effect of nano-graphene oxide on shear bond strength of conventional and resin-modified glass ionomer cement. Clin Exp Dent Res 2023;9:851-858. PUBMED | CROSSREF
30. Bahammam S, Nathanson D, Fan Y. Evaluating the mechanical properties of restorative glass ionomers cements. Int Dent J 2022;72:859-865. PUBMED | CROSSREF
31. Hussein TA, Bakar WZ, Ghani ZA, Mohamad D. The assessment of surface roughness and microleakage of eroded tooth-colored dental restorative materials. J Conserv Dent 2014;17:531-535. PUBMED | CROSSREF
32. de Camargo FLL, Lancellotti AC, de Lima AF, Geraldo Martins VR, Gonçalves LS. Effects of a bleaching agent on properties of commercial glass-ionomer cements. Restor Dent Endod 2018;43:e32. PUBMED | CROSSREF
33. Tsuge T. Radiopacity of conventional, resin-modified glass ionomer, and resin-based luting materials. J Oral Sci 2009;51:223-230. PUBMED | CROSSREF
34. Carvalho-Junior JR, Correr-Sobrinho L, Correr AB, Sinhoreti MA, Consani S, Sousa-Neto MD. Solubility and dimensional change after setting of root canal sealers: a proposal for smaller dimensions of test samples. J Endod 2007;33:1110-1116. PUBMED | CROSSREF
35. Shintome LK, Nagayassu MP, Di Nicoló R, Myaki SI. Microhardness of glass ionomer cements indicated for the ART technique according to surface protection treatment and storage time. Braz Oral Res 2009;23:439-445. PUBMED | CROSSREF
36. Buldur M, Sirin Karaarslan E. Microhardness of glass carbomer and high-viscous glass ionomer cement in different thickness and thermo-light curing durations after thermocycling aging. BMC Oral Health 2019;19:273. PUBMED | CROSSREF
37. Eshaghi Gorji F, Seyedmajidi M, Asgharpours F, Tashakorian H, Moghadamnia AA, Kazemi S, *et al*. Oral mucosa and *Streptococcus mutans* count in the saliva. Does graphene oxide nanoparticle mouthwash have a good effect? Caspian J Intern Med 2021;12:342-349. PUBMED | CROSSREF
38. He J, Zhu X, Qi Z, Wang C, Mao X, Zhu C, *et al*. Killing dental pathogens using antibacterial graphene oxide. ACS Appl Mater Interfaces 2015;7:5605-5611. PUBMED | CROSSREF
39. Mao M, Zhang W, Huang Z, Huang J, Wang J, Li W, *et al*. Graphene oxide-copper nanocomposites suppress cariogenic *Streptococcus mutans* biofilm formation. Int J Nanomedicine 2021;16:7727-7739. PUBMED | CROSSREF
40. Zhao M, Shan T, Wu Q, Gu L. The antibacterial effect of graphene oxide on *Streptococcus mutans*. J Nanosci Nanotechnol 2020;20:2095-2103. PUBMED | CROSSREF
41. Hegab HM, ElMekawy A, Barclay TG, Michelmore A, Zou L, Saint CP, *et al*. Single-step assembly of multifunctional poly(tannic acid)-graphene oxide coating to reduce biofouling of forward osmosis membranes. ACS Appl Mater Interfaces 2016;8:17519-17528. PUBMED | CROSSREF
42. Zhou R, Gao H. Cytotoxicity of graphene: recent advances and future perspective. Wiley Interdiscip Rev Nanomed Nanobiotechnol 2014;6:452-474. PUBMED | CROSSREF
43. Simón-Soro A, Mira A. Solving the etiology of dental caries. Trends Microbiol 2015;23:76-82. PUBMED | CROSSREF
44. Hitij T, Fidler A. Radiopacity of dental restorative materials. Clin Oral Investig 2013;17:1167-1177. PUBMED | CROSSREF
45. ADA Division of Science, ADA Council on Scientific Affairs. Resin-based composites. J Am Dent Assoc 2003;134:510-512. PUBMED | CROSSREF
46. Willems G, Noack MJ, Inokoshi S, Lambrechts P, Van Meerbeek B, Braem M, *et al*. Radiopacity of composites compared with human enamel and dentine. J Dent 1991;19:362-365. PUBMED | CROSSREF
47. Espelid I, Tveit AB, Erickson RL, Keck SC, Glasspoole EA. Radiopacity of restorations and detection of secondary caries. Dent Mater 1991;7:114-117. PUBMED | CROSSREF
48. Sidhu SK, Shah PM, Chong BS, Pitt Ford TR. Radiopacity of resin-modified glass-ionomer restorative

cements. Quintessence Int 1996;27:639-643. PUBMED

49. Prévost AP, Forest D, Tanguay R, DeGrandmont P. Radiopacity of glass ionomer dental materials. Oral Surg Oral Med Oral Pathol 1990;70:231-235. PUBMED | CROSSREF
50. Yaylacı A, Karaarslan ES, Hatırlı H. Evaluation of the radiopacity of restorative materials with different structures and thicknesses using a digital radiography system. Imaging Sci Dent 2021;51:261-269. PUBMED | CROSSREF
51. Aydın N, Karaoğlanoğlu S, Aybala-Oktay E, Çetinkaya S, Erdem O. Investigation of water sorption and aluminum releases from high viscosity and resin modified glass ionomer. J Clin Exp Dent 2020;12:e844-e851. PUBMED | CROSSREF
52. Müller JA, Rohr N, Fischer J. Evaluation of ISO 4049: water sorption and water solubility of resin cements. Eur J Oral Sci 2017;125:141-150. PUBMED | CROSSREF
53. Brito CR, Velasco LG, Bonini GA, Imparato JC, Raggio DP. Glass ionomer cement hardness after different materials for surface protection. J Biomed Mater Res A 2010;93A:243-246. PUBMED | CROSSREF
54. Sun J, Zhao J. Multi-layer graphene reinforced nano-laminated WC-Co composites. Mater Sci Eng A 2018;723:1-7. CROSSREF
55. Siddique R, Mehta A. Effect of carbon nanotubes on properties of cement mortars. Constr Build Mater 2014;50:116-129. CROSSREF
56. Asmussen E, Peutzfeldt A. Long-term fluoride release from a glass ionomer cement, a compomer, and from experimental resin composites. Acta Odontol Scand 2002;60:93-97. PUBMED | CROSSREF
57. Nassar HM, Platt JA. Fluoride release from two high-viscosity glass ionomers after exposure to fluoride slurry and varnish. Materials (Basel) 2019;12:3760. PUBMED | CROSSREF
58. Seppä L, Forss H, Ogaard B. The effect of fluoride application on fluoride release and the antibacterial action of glass ionomers. J Dent Res 1993;72:1310-1314. PUBMED | CROSSREF
59. Cury JA, de Oliveira BH, dos Santos AP, Tenuta LM. Are fluoride releasing dental materials clinically effective on caries control? Dent Mater 2016;32:323-333. PUBMED | CROSSREF
60. Hicks J, Garcia-Godoy F, Donly K, Flaitz C. Fluoride-releasing restorative materials and secondary caries. J Calif Dent Assoc 2003;31:229-243. PUBMED | CROSSREF